

Recent advances in organic, inorganic, andhybrid thermoelectric aerogels

Lirong Liang(梁丽荣), Xiaodong Wang(王晓东), Zhuoxin Liu(刘卓鑫),Guoxing Sun(孙国星), and Guangming Chen(陈光明)

Citation: Chin. Phys. B, 2022, 31 (**2**): 027903. DOI: 10.1088/1674-1056/ac2802

Journal homepage: http://cpb.iphy.ac.cn; http://iopscience.iop.org/cpb

What follows is a list of articles you may be interested in

Thermoelectric enhancement in triple-doped strontium titanate with multi-scale microstructure

Zheng Cao(曹正), Qing-Qiao Fu(傅晴俏), Hui Gu(顾辉), Zhen Tian(田震), Xinba Yaer(新巴雅尔), Juan-Juan Xing(邢娟娟), Lei Miao(苗蕾), Xiao-Huan Wang(王晓欢), Hui-Min Liu(刘慧敏), and Jun Wang(王俊)

Chin. Phys. B, 2021, 30 (**9**): 097204. DOI: 10.1088/1674-1056/abe9a9

First principles calculations on the thermoelectric properties of bulk Au_2S with ultra-low lattice thermal conductivity

Y Y Wu(伍义远), X L Zhu(朱雪良), H Y Yang(杨恒玉), Z G Wang(王志光), Y H Li(李玉红), B T Wang(王保田)

Chin. Phys. B, 2020, 29 (**8**): 087202. DOI: 10.1088/1674-1056/ab973c

Electrically tunable spin diode effect in a tunneling junction of quantum dot

Xukai Peng(彭许凯), Zhengzhong Zhang(张正中)

Chin. Phys. B, 2019, 28 (**12**): 127202. DOI: 10.1088/1674-1056/ab53d0

The magneto-thermoelectric effect of graphene with intra-valley scattering

Wenye Duan(段文晔), Junfeng Liu(刘军丰), Chao Zhang(张潮), Zhongshui Ma(马中水)

Chin. Phys. B, 2018, 27 (**9**): 097204. DOI: 10.1088/1674-1056/27/9/097204

Complex alloying effect on thermoelectric transport properties of $Cu_2Ge(Se_{1-x}Te_x)_3$

Ruifeng Wang(王瑞峰), Lu Dai(戴璐), Yanci Yan(闫艳慈), Kunling Peng(彭坤岭), Xu Lu(卢旭), Xiaoyuan Zhou(周小元), Guoyu Wang(王国玉)

Chin. Phys. B, 2018, 27 (**6**): 067201. DOI: 10.1088/1674-1056/27/6/067201

TOPICAL REVIEW — Organic and hybrid thermoelectrics

Recent advances in organic, inorganic, and hybrid thermoelectric aerogels

Lirong Liang(梁丽荣)[1], Xiaodong Wang(王晓东)[2], Zhuoxin Liu(刘卓鑫)[2,†], Guoxing Sun(孙国星)[1,‡], and Guangming Chen(陈光明)[2,§]

[1] *Joint Key Laboratory of the Ministry of Education, Institute of Applied Physics and Materials Engineering, University of Macau, Avenida da Universidade, Taipa, SAR, Macau, China*

[2] *College of Materials Science and Engineering, Shenzhen University, Shenzhen* 518055, *China*

(Received 28 August 2021; revised manuscript received 12 September 2021; accepted manuscript online 18 September 2021)

The thermoelectric (TE) materials and corresponding TE devices can achieve direct heat-to-electricity conversion, thus have wide applications in heat energy harvesting (power generator), wearable electronics and local cooling. In recent years, aerogel-based TE materials have received considerable attention and have made remarkable progress because of their unique structural, electrical and thermal properties. In this review, the recent progress in both organic, inorganic, and composite/hybrid TE aerogels is systematically summarized, including the main constituents, preparation method, TE performance, as well as factors affecting the TE performance and the corresponding mechanism. Moreover, two typical aerogel-based TE devices/generators are compared and analyzed in terms of assembly modes and output performance. Finally, the present challenges and some tentative suggestions for future research prospects are provided in conclusion.

Keywords: thermoelectric materials, thermoelectric device, aerogel, thermoelectric performance

PACS: 79.10.−n, 72.15.Jf, 84.60.Rb **DOI:** 10.1088/1674-1056/ac2802

1. Introduction

Thermoelectric (TE) materials and corresponding TE devices that can directly achieve the heat-to-electricity conversion are attracting tremendous interests as a next-generation power generator and a promising power source for various external powered electronics.[1–4] The TE devices exhibit some unique merits over other energy devices, such as no vibration, no liquid/gas emission, no noise, easy maintenance and long operating lifetime.[5,6] To evaluate the TE performance of materials, a dimensionless figure of merit ZT ($ZT = S^2\sigma T/\kappa$, where S is the Seebeck coefficient that derived from the generated thermovoltage (ΔV) when a temperature difference (ΔT) is applied to the material, σ and κ are the electrical conductivity and thermal conductivity, respectively, and T is the absolute temperature) is usually adopted. Moreover, for some organic TE materials and their composites, power factor ($PF = S^2\sigma$) is directly applied to evaluate their TE performance owing to the intrinsic low κ of their organic polymer constituents.[3,7–9] Therefore, to achieve a desired ZT value, a high σ, a large S and a low κ should be obtained simultaneously. However, there is a strong trade-off among these three parameters, resulting in difficulties to simultaneously improve them.[3,7]

Conventional inorganic TE materials, emerging organic TE materials, and the composite/hybrid TE materials have received extensive attentions due to their respective merits.[2,5,8] Among them, inorganic TE materials such as Bi_2Te_3, Sb_2Te_3 and PbTe reveal relatively high ZT values because of their large S, resulting in their great potential in practical applications.[8,10–12] However, their high cost, toxicity, poor processability, scare resources, together with the intrinsic rigidity seriously keep them from wide application.[3,7] Meanwhile, despite the lower ZT values, organic TE materials, particularly conjugated conducting polymers, can circumvent these difficulties because of their various advantages of low cost, rich resources, easy synthesis, intrinsic low κ, good solution-processability and adjustable molecular structure, making them highly competitive candidates for a new generation of TE materials.[6,13–15] Moreover, composite/hybrid TE materials including pure inorganic TE composites,[16] pure organic TE composites[17,18] as well as organic/inorganic TE composites,[7,10,19–23] where the inorganic constituents mainly include inorganic semiconductor TE materials,[5,24] carbon nanoparticles[25–27] and some metal nanoparticles,[28–30] and the organic constituents are mainly those conducting polymers and some insulating polymers (polyurethane,[4] polyvinyl alcohol,[31,32] polycarbonate,[33] etc), have been developed. Such combination is intended to further enhance TE properties (high σ and S, low κ), to improve flexibility (stretching, bending, folding, compressing) and/or to endow them with other

†Corresponding author. E-mail: liuzhuoxin@szu.edu.cn
‡Corresponding author. E-mail: gxsun@um.edu.mo
§Corresponding author. E-mail: chengm@szu.edu.cn

© 2022 Chinese Physical Society and IOP Publishing Ltd

functions (magnetism, responsiveness, etc).[1,4,8]

However, these TE materials mainly exist in the form of films or solid bulks,[1,3,10] limiting their applications as elastic and compression-driven response TE materials. Aerogel, a three-dimensional (3D) porous material with a large surface area and a high porosity, has shown successfully applications in electronic devices (sensor, electrode), energy storage, catalysis, heat insulator, and detectors.[34–36] Considering the advantage of ultralow κ that originates from their high void volume (high porosity), aerogel-based TE materials can be optimized simultaneously in structure and TE performance.[37,38] In the last few years, the construction of TE aerogels with unique structural, electrical and thermal properties based on the above organic, inorganic and composite/hybrid TE materials has been extensively studied. Unfortunately, although aerogel-based TE materials have made remarkable achievements and become a novel research topic in TE materials, we note that there has been no review of TE aerogels so far, especially compared with various reviews reported on advances in films or solid bulk materials of TE materials.[3,8,39,40]

In this review, we focus on the introduction of the recent progress of organic, inorganic and their composite/hybrid TE aerogels, including the main constituents, preparation method, TE performance, as well as factors affecting the TE performance and the corresponding mechanism. Subsequently, some representative aerogel-based TE devices/generators including their assembly mode and TE output performance analysis are presented. Finally, a brief conclusion and prospects for this emerging field are provided.

2. Research progress of organic, inorganic and hybrid TE aerogels

It is well known that organic polymers possess extremely low κ, demonstrating their promising application in TEs.[3,14] Meanwhile, carbon nanoparticles are usually used as fillers in organic polymer matrix to endow the resultant composites with both optimized TE performance and excellent mechanical property (flexibility, stretchability and compressibility).[8,39] Besides, some inorganic semiconductors[21,41] with large S and metal particles[28,29] with intrinsically high σ are also employed to improve the TE properties of organic polymers. Herein, we will introduce and discuss the recent advances of organic, inorganic and some hybrid/composite TE aerogels.

2.1. Organic TE aerogels

Various conjugated conducting polymers have been widely studied in fields of solar cells, capacitors, sensors, electrodes as well as thermoelectrics.[2,42–44] Among them, poly(3,4-ethylenedioxythiophene): poly(4-styrenesulfonate) (PEDOT:PSS) exhibits unique advantages in achieving efficient TE energy conversion owing to its adjustable σ, solution processing ability and good environmental stability.[45] To further improve its TE properties, some organic solvents (ethylene glycol (EG), dimethyl sulfoxide (DMSO), methanol) are usually used as de-doping/doping agents by removing some insulating PSS, changing the conformation of the polymer chains from coil to linear, increasing carriers concentration, tuning carriers transportation, etc.[44,46] Combing the excellent TE performance of conducting polymers with the desired mechanical structure of aerogel, the conducting polymer based aerogels are highly promising candidates to construct practically soft/elastic/ultralight TE devices.[35,47–49] The TE properties of some typical organic TE aerogels are summarized in Table 1.

For instance, Urban *et al.* reported for the first time a pure PEDOT:PSS TE aerogel prepared without additional crosslinking agents via a facile freeze-drying and followed by EG treatment approach.[47] In detail, it includes three main steps: PEDOT:PSS thick film, rehydrate and freeze-drying, as shown in Fig. 1(a). For their TE performance, consistent with previous reports on PEDOT:PSS films, the aerogel revealed an obviously enhanced σ originating from the emergence of large-scale PEDOT-rich domains on the surface by removing part of PSS. [46] In contrast, the PEDOT:PSS aerogel presented unchanged S after EG treatment, which was attributed to the structural change of polymer network instead of the change of carriers concentration. Unexpectedly, the TE property of the prepared aerogel was insensitive to the macroscale geometry of the polymeric material, which means the aerogel had the same PF as the film sample. Subsequently, Jiang *et al.* studied TE properties of PEDOT:PSS aerogel films pretreated with various organic solvents, where they found a porous network and a conformation transition (benzoid type to quinoid type) of PEDOT:PSS after NMP addition, which resulted in a large PF of 1.24 $\mu W \cdot m^{-1} \cdot K^{-2}$.[35] To alleviate the shrinkage problems caused by pre- or post-treatment of PEDOT:PSS aerogels, Shimomura *et al.* adopted a second doping in supercritical CO_2 ($ScCO_2$) atmosphere with methanol to the freeze-dried aerogels, and the results showed an obviously improved σ and S.[48] Besides PEDOT:PSS, they conducted the TE aerogel pioneer work of the incorporation of poly(3-hexylthiophene) (P3HT) conducting nanofibers with polystyrene (PS).[49] In detail, the P3HT/PS composite aerogels were prepared according to a three-step method, which involved the formation of P3HT nanofibers dispersions in PS and p-xylene solutions, freeze-drying and the subsequent doping with iodine vapor, as shown in Fig. 1(b). Resultantly, the composite aerogels achieved a giant $S > 10$ $mV \cdot K^{-1}$ that attributed to the unique structure consisting of a thin PS sheet embedded with entangled P3HT nanofibers and the effect of energy filtering. However, this composite aerogels revealed a low σ of 8×10^{-5} $S \cdot cm^{-1}$, thus generating a ZT value of 7×10^{-3}.

Table 1. The summary of TE performances for organic aerogels.

Constituent (solvent treatment)	κ (W·m^{-1}·K^{-1})	S (μV·K^{-1})	σ (S·cm^{-1})	PF (μW·m^{-1}·K^{-2})	ZT	Ref.
PEDOT:PSS aerogel (EG)	–	∼ 19	∼ 190	6.86	–	[47]
PEDOT:PSS-H_2O aerogel film (DMSO)	$\kappa_{||}$0.14	28	0.5	0.04	–	[35]
PEDOT:PSS-NMP aerogel film	$\kappa_{||}$0.14	18.8	35	1.24	–	[35]
PEDOT:PSS aerogel	0.03	13	2.06×10^{-4}	3.47×10^{-6}	3.54×10^{-8}	[48]
PEDOT:PSS aerogel (methanol)	0.2	17	2.35	0.07	9×10^{-4}	[48]
P3HT/PS (iodine vapour)	0.03	$> 1 \times 10^4$	8×10^{-5}	0.68	7×10^{-3}	[49]

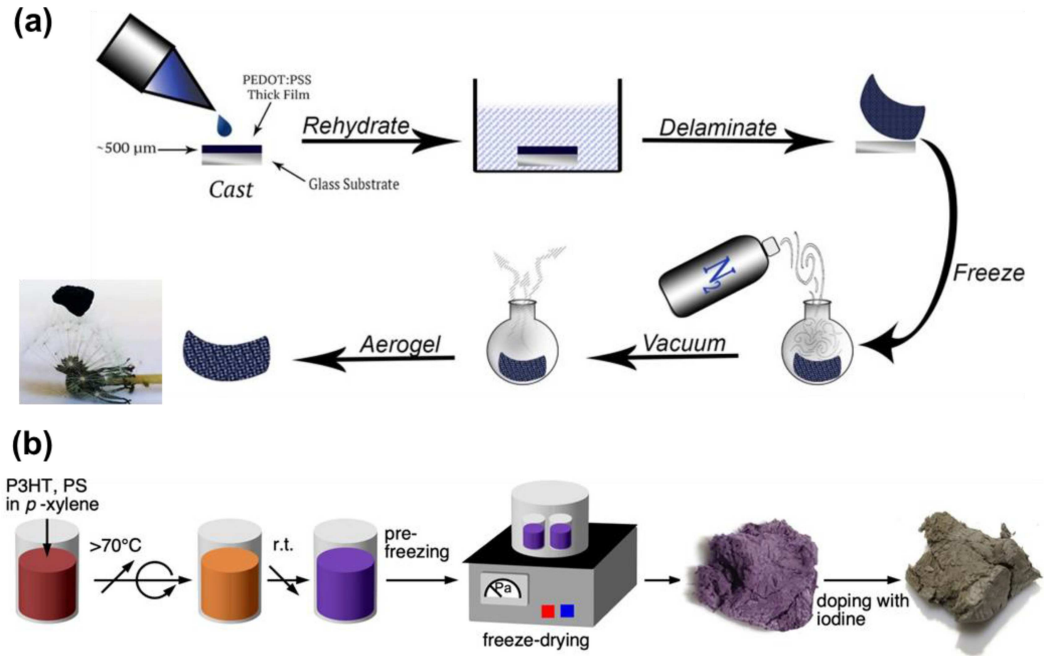


Fig. 1. (a) Schematic illustration of the preparation process of PEDOT:PSS thick films and aerogels. Reproduced with permission.[47] Copyright 2016, John Wiley and Sons. (b) Schematic synthesis of freeze-dried P3HT nanofiber/PS aerogels. Reproduced with permission.[49] Copyright 2020, American Chemical Society.

2.2. Inorganic TE aerogels

Traditional TE materials are mainly based on inorganic semiconductors and their alloys, such as Bi_2Te_3, PbTe, Sb_2Te_3, etc.[12,45] Considering the attractive structural features of aerogel, the construction of inorganic TE material based aerogel is expected to further improve its TE performance. For instance, Brock *et al.* reported two kinds of aerogels, Bi_2Te_3 and $Bi_xSb_{2-x}Te_3$, prepared by discrete thiolate-capped nanoparticles with a sol-gel methodology, and followed by $ScCO_2$ drying process.[51] Figure 2 shows the image of Bi_2Te_3 aerogel, wet gel, and sol. The resulting aerogels showed a unique 3D porous network and a significantly enhanced surface area (Fig. 2). Unexpectedly, their PF were reduced with respect to the corresponding bulk materials. The authors attributed such reduction to the transition between two types of majority carries (electrons and holes) in Bi_2Te_3 aerogels and the presence of excess Te in the $Bi_xSb_{2-x}Te_3$ aerogels. For their lattice κ, Bi_2Te_3 aerogel revealed a reduced value, while the $Bi_xSb_{2-x}Te_3$ aerogel exhibited a similar value, as compared to their respective nanoparticles. Therefore, optimizing the carrier concentration of the aerogels is needed to further improve their TE performance.

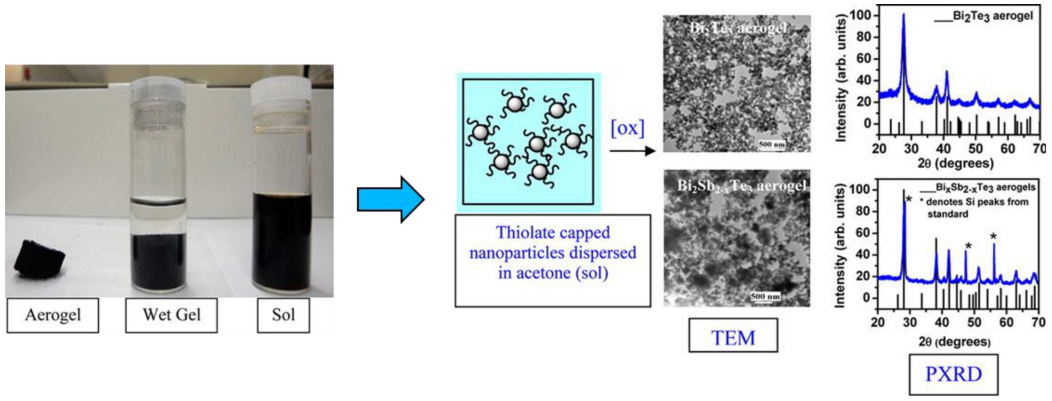


Fig. 2. Image photos of Bi_2Te_3 aerogel, wet gel, and sol. The morphology and structure characterization of the prepared Bi_2Te_3 and $Bi_xSb_{2-x}Te_3$ aerogel. Reproduced with permission.[51] Copyright 2012, American Chemical Society.

Besides inorganic TE materials, carbon nanoparticles-based (carbon nanotubes (CNTs), graphene, reduced graphene oxide (rGO), graphene oxide (GO)) materials have been widely studied in various areas of bioelectronics, catalysis, electrodes, sensors, energy storage as well as thermoelectronics.[3,52] Considering the relatively high κ of carbon nanoparticles, the construction of 3D aerogels can effectively increase the porosity and thus reduce their κ, and this favorable effect will facilitate the TE energy conversion. For instance, Chen *et al*. adopted a chemical vapour deposition (CVD) method to prepare the pure 3D CNT aerogels, and results showed that the CNT aerogel revealed an extremely low κ of 0.02 $\mathrm{W{\cdot}m^{-1}{\cdot}K^{-1}}$ because of its high porosity (low density) of the unique 3D framework structure.[53] However, their σ and S were not superior to other CNT films/sheets, thus leading to a poor PF of 0.04 $\mu\mathrm{W{\cdot}m^{-1}{\cdot}K^{-2}}$. More interestingly, they found that the doping treatment by gas fuming method with potassium (K) and iodine (I_2) can adjust the electrical transportation of the CNT aerogel. Resultantly, the p-type CNT aerogel transformed to n-type after K doping, whereas I_2 doping obviously improved its σ.

Due to the unique synergistic effect of 1D CNT and 2D graphene sheets, it is highly beneficial to prepare hybrid aerogels to further enhance their mechanical and TE properties. Li *et al.* presented a graphene/MWCNT composite aerogel fabricated via a three-step process: the preparation of graphene oxide/MWCNT aqueous dispersion, freeze-drying and the followed pyrolysis.[54] This composite aerogel revealed obviously increased σ and S with the MWCNT:GO mass ratio lower than 0.8. Resultantly, at MWCNT:GO mass ratio of 0.5, the ZT reached a peak value of 0.001, which was attributed to the optimization of electron transportation, the energy filtering effect as well as the phonon scattering in the 3D porous skeleton structure. More recently, Meek *et al.* prepared the rGO/MWCNTs hybrid aerogels via a hydrothermal-solvothermal and subsequent freeze-drying process.[55] Similarly, the increase of MWCNTs content effectively optimized the TE properties (σ and S) of the hybrid aerogels. Compared with MWCNT, SWCNT has higher σ and structural advantages, which has also been confirmed in some composite TE materials. Therefore, the preparation of composite aerogels combined with SWCNT is expected to further improve their TE and mechanical properties. In 2016, our group has successfully hybridized rGO with SWCNT to achieve the preparation of ultralight rGO/SWCNT hybrid aerogels with a 3D double-interconnected network porous structure.[56] This hybrid aerogel was prepared through the formation of well-dispersed structure in the GO/SWCNT hybrid hydrogels, freezing-thawing recycle, and the final reduction and freeze-drying process (Fig. 3). Notably, the obtained hybrid aerogels revealed highly reversible deformation during the mechanical compression process ($\varepsilon = 0$–40%), where the σ significantly increased (6.66–11.5 $\mathrm{S{\cdot}cm^{-1}}$) and their S can be well-reserved (29–25.6 $\mu\mathrm{V{\cdot}K^{-1}}$). A ZT value of 8.03×10^{-3} was obtained at zero compressive strain, resulting from the unique 3D double-interconnected network, and the assistance of energy-filtering and the phonon-scattering effect.

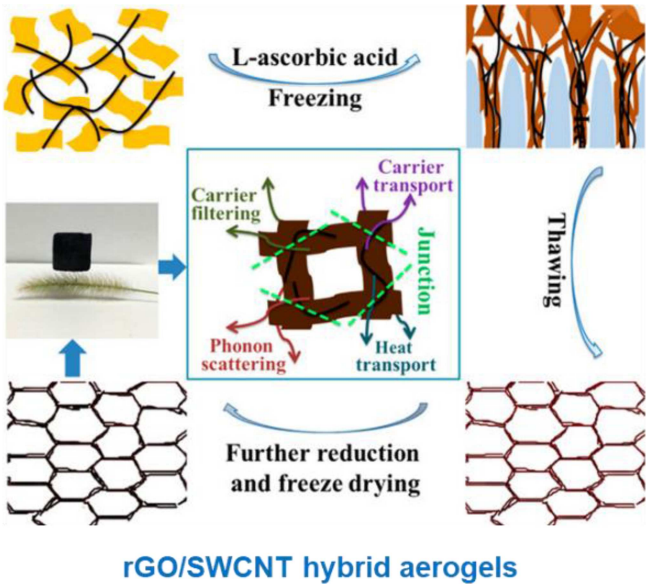


Fig. 3. Schematic illustration of the synthesis route of the rGO/SWCNT hybrid aerogels. Reproduced with permission.[56] Copyright 2017, American Chemical Society.

For conducting carbon composite aerogels, they can also obtained through composite with some other inorganic constituents, such as some highly conductive metal particles and carbon particles (C) originate from pyrolyzed organic polymers.[57,58] For instance, Zhao *et al.* obtained a graphene/C hybrid aerogel (GHCAs) by introducing graphene into the pyrolyzed resorcinol-formaldehyde (RF) aerogel.[57] It exhibited a dramatically enhanced ZT value of 0.01 at graphene weight content of 39 wt%. They attributed the excellent TE performance to the energy filtering effect (large S) and the compact 3D network with tight junctions (high σ), as well as the effective phonon scattering effect (ultralow κ). In another study, they reported the CNT/Ag composite aerogels fabricated by a four-step method, including the formation of CNT/Ag dispersions, the preparation of CNT/Ag+RF composite hydrogel, freeze-drying and finally pyrolysis process.[58] It exhibited a large PF of 2.683 $\mu\mathrm{W{\cdot}m^{-1}{\cdot}K^{-2}}$ at 42.56 wt% Ag content with a relatively low κ of 0.077 $\mathrm{W{\cdot}m^{-1}{\cdot}K^{-1}}$, leading to a high ZT value of 0.011, which was one of the highest reported values in inorganic-based TE aerogels. Similarly, the enhanced TE performance was attributed to the simultaneously increased σ and S, as well as maintain low κ.

In order to conveniently analyze and compare the TE performance of inorganic-based aerogels, we summarized their TE properties in Table 2.

Table 2. Summary of the TE properties for inorganic aerogels.

Constituent (experimental condition)	κ (W·m^{-1}·K^{-1})	S (μV·K^{-1})	σ (S cm^{-1})	PF (μW·m^{-1}·K^{-2})	ZT (300 K)	Ref.
Bi_2Te_3 aerogel	0.5	43	30.3	6	3×10^{-3}	[51]
$Bi_xSb_{2-x}Te_3$ aerogel	1	−36	133.33	17.27	3×10^{-3}	[51]
CNT	0.02	18.2	1.23	0.04	6×10^{-4}	[53]
CNT (K)	–	−12.5	1.1	0.017	–	[53]
CNT (I_2)	–	20.5	2.97	0.125	–	[53]
Graphene/MWCNT	0.056	58	0.52	0.175	1×10^{-3}	[54]
rGO/MWCNTs	–	15 ($\Delta T = 80$ K)	–	1	–	[55]
rGO/SWCNT	0.021	29	6.66	0.56	8.03×10^{-3}	[56]
rGO/SWCNT ($\varepsilon = 40\%$)	–	25.6	11.5	0.754	–	[56]
Graphene/C	0.064	82	3.25	2.185	1.02×10^{-2}	[57]
CNT/Ag	0.077	54	9.2	2.683	1.1×10^{-2}	[58]

2.3. Organic/inorganic particle hybrid/composite TE aerogels

Given the distinct advantages of inorganic-based aerogels, it is highly beneficial to combine them with organic polymers to impart the resultant composite aerogels with both high TE property and freely shapeable property (elasticity, compressibility, stretchability, flexibility, etc).[37,59–62] The TE properties of some typical organic/inorganic particle hybrid TE aerogels are summarized in Table 3. For instance, Yao *et al.* fabricated a PANI/3D graphene composite aerogel via a convenient *in situ* polymerization with 3D tubular graphene as skeleton.[59] This composite aerogel with 55 wt% 3D graphene possessed the highest PF of 13.2 μW·m^{-1}·K^{-2}, leading to a high ZT value of 0.02. Similarly, Chen *et al.* obtained an elastic PANI/3D CNT composite aerogel using 3D CNT network as template to composite with PANI, as illustrated in Fig. 4(a).[53] However, it exhibited a ZT value of 2.2×10^{-3}, much lower than that of PANI/3D graphene composite aerogels. Considering the high S of inorganic semiconductor Te nanowires (Te-NWs), Jiang *et al.* prepared the PEDOT:PSS/Te-NWs binary aerogels via the formation of PEDOT:PSS and Te-NWs dispersion, vacuum freeze drying and subsequent DMSO-vapor annealing process, as illustrated in Fig. 4(b).[35] Notably, they only studied the TE performance of PEDOT:PSS/Te-NWs binary aerogel films by pressing the aerogel samples. This aerogel film with 30 wt% Te-NWs exhibited a high PF of 13.2 μW·m^{-1}·K^{-2} and a ZT value of 0.02. The authors explained such enhancement in TE performance with a binary composite model (series and parallel connected model).

Besides the ultralow κ, the reversible elasticity (deformation) under different compression strains of aerogel is also a distinct advantage to broaden its application. More recently, Cho *et al.* investigated the TE property of SWCNT-coated polyurethane (PU) aerogel (or sponge) prepared by a convenient dipping-and-drying process.[38] Notably, the obtained TE aerogels exhibited highly compressible, elastic, flexible, bendable and twistable features, which completely inherited the pristine excellent mechanical properties of the PU sponge. Given the above attractive mechanical properties, they further investigated their TE performances under different compressive strains (ε = 0–80%). Unsurprisingly, both σ (0.028–0.073 S·cm^{-1}) and κ (0.055–0.08 W·m^{-1}·K^{-1}) increased with the increase of compressive strain (ε = 0–80%) because of the optimization of the conductive pathway by reducing the pore size (increasing the density), while their S (37.05–38.91 μV·K^{-1}) can be well maintained. As a result, their ZT values were largely improved from 1.74×10^{-5} to 3.86×10^{-5} under the compressive strain from 40% to 80%. More importantly, they also constructed a TE generator to evaluate their output performance in practical application, as introduced in the following Section 3.

Ternary polymers and carbon nanoparticles composite aerogels have also been developed for TE applications. As reported by Zhao's group, an ultralight PEDOT:PSS/MWCNTs/Ag ternary composite aerogel was prepared via a facile route of the formation of ternary dispersion and subsequent freeze-drying process.[61] At 33.32 wt% Ag loading, the ZT reached a peak value of 7.6×10^{-3}, which is one order of magnitude higher than that of the

Table 3. Summary of the TE properties for organic/inorganic hybrid aerogels.

Constituent (solvent treatment)	κ (W·m^{-1}·K^{-1})	S (μV·K^{-1})	σ (S·cm^{-1})	PF (μW·m^{-1}·K^{-2})	ZT	Ref.
PANI/3D graphene	0.198	37.5	92	13.2	0.02	[59]
PANI/ 3D CNT	0.29	23.3	40.35	2.19	2.2×10^{-3}	[33]
PEDOT:PSS/GO	0.035	10	–	–	–	[60]
PEDOT:PSS/Te-NWs aerogel film (DMSO)	0.168	30.8	119	11.3	0.02	[35]
SWCNT-coated PU sponge	0.055	37.05	0.028	3.84×10^{-3}	2.09×10^{-5}	[38]
SWCNT-coated PU sponge ($\varepsilon = 80\%$)	0.08	38.91	0.073	0.011	3.86×10^{-5}	[38]
PEDOT:PSS/MWCNTs/Ag (DMSO)	0.12	61.3	6.71	2.52	7.6×10^{-3}	[61]
PEDOT:PSS/SWCNT/BC aerogel film	0.13	20.29	290.6	12	0.028	[37]

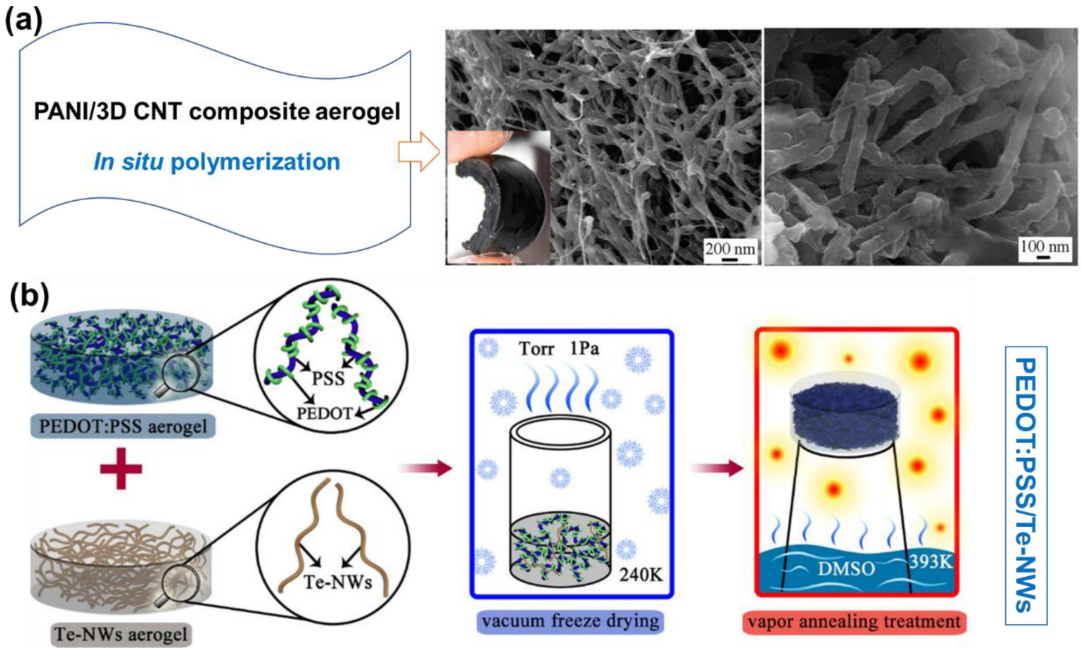


Fig. 4. Schematic illustration showing the preparation process for the (a) PANI/3D CNT composite aerogel. Reproduced with permission.[53] Copyright 2011, American Chemical Society. (b) PEDOT:PSS/Te-NWs aerogel film. Reproduced with permission.[35] Copyright 2018, American Chemical Society.

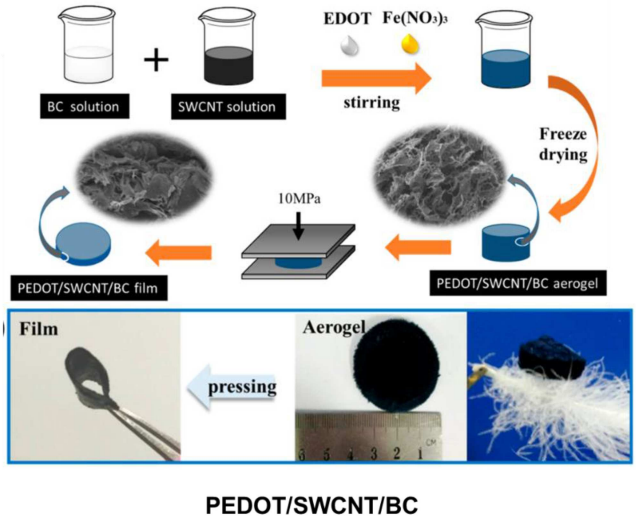


Fig. 5. Synthesis route of the PEDOT/SWCNT/BC ternary composite aerogels respectively. Reproduced with permission.[37] Copyright 2019, American Chemical Society.

pristine PEDOT:PSS/MWCNTs aerogel. Such enhancement of TE properties was also ascribed to the unique 3D porous conductive network, the energy-filtering effect, and the effective phonon scattering effect at the aerogel interface. Furthermore, Lin *et al.* obtained a ternary PEDOT/SWCNT/BC composite aerogel, which exploits the high σ from PEDOT and SWCNT, and the beneficial mechanical properties from bacterial cellulose (BC).[37] The ternary composite aerogel was prepared through the formation of SWCNT/BC dispersion, *in situ* polymerization of PEDOT and subsequent freeze-drying process, as shown in Fig. 5. In order to compensate for the ultralow σ caused by high porosity, the obtained aerogels were cold-pressed into corresponding films, and then their TE performance were investigated. At the SWCNT mass content of 32%, the aerogel film exhibited an extremely high σ of 290.6 S·cm^{-1}, which was 9.7 times that of the SWCNT/BC (32 wt%) film and 53 times that of the PEDOT/BC film. Moreover, the κ can be well-controlled at 0.13 W·m^{-1}·K^{-1}, thus leading to a high ZT value of 0.028.

3. Flexible TE devices based on TE aerogels

To further explore the practicality of the TE materials, corresponding TE devices or generators are required, which are assembled in plane or vertical plane mode from TE modules that are composed of p-type and/or n-type TE materials. For in-plane design, films are the most commonly used structure for flexible TE devices. Therefore, the resulting 3D aerogel is sometimes cold-pressed into a film. Compared with 3D aerogel and pristine film sample, the corresponding aerogel film has three distinct merits: 1) enhanced σ due to the optimization of conductive transport pathway, 2) maintained relatively low κ because of the remaining pores, 3) convenient TE property and output performance measurements, particularly for those aerogels with poor mechanical properties. For instance, Jiang *et al.* constructed a TE generator by connecting 6 pairs of prepared p-type PEDOT:PSS/Te-NWs (DMSO) aerogel films and matching n-type CNT fibers in series.[35] As shown in Fig. 6(a), the TE generator achieved a high output power of 1.28 μW at a temperature difference (ΔT) of 60 K, which was 2 times that of TE generator consisting of aerogel films without DMSO post-treatment. Moreover, Lin *et al.* reported an in-plane flexible TE device which composed of 10 unipolar p-type legs of PEDOT /SWCNT/BC composite aerogel films, as shown in Fig. 6(b).[37] Resultantly, as ΔT increased to 65.6 K, the TE device generated a maximum open circuit voltage of 6.9 mV, thus leading to a largest output power of 169 nW.

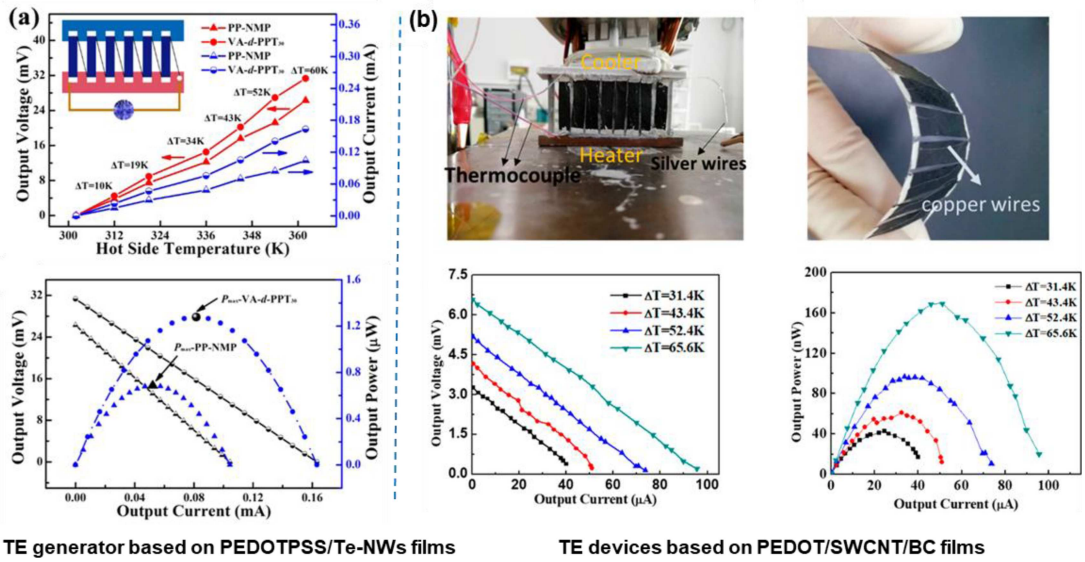


Fig. 6. The output performance of the TE devices based on (a) PEDOT:PSS/Te-NWs aerogel films (Reproduced with permission.[35] Copyright 2018, American Chemical Society) and (b) PEDOT/SWCNT/BS aerogel films (Reproduced with permission.[37] Copyright 2019, American Chemical Society).

To exploiting large-area heat sources and achieving wearable applications, vertical-plane design of TE devices is the most desired structure to efficiently harness thermal energy via vertical temperature gradient. This vertical design is particularly suitable for 3D bulk aerogels. For example, Cho *et al.* fabricated an elastic TE generator via the assembly of 8 pains of p-type SWCNT coated-PU sponge legs ($FeCl_3$ doping) and n-type SWCNT coated-PU sponge legs (benzyl viologen doping).[38] The legs were cut into a specific size and then embedded in a perforated PU sponge mold. Notably, this generator exhibited a considerable stable and durable relative resistance change during continuous compression–release for 1000 cycles, confirming its excellent pressure-driven response. Considering the super elasticity and sensitive compression-driven response, their changes in output performance of the generator depending on compression strains were also investigated. The TE sponge generator revealed a remarkable output power of 2.09 μW under 80% strain at $\Delta T = 55$ K, which was around 12 times that of TE generator without strain. This elastic TE generator was further demonstrated to be cushion on human body, generating an S of 10 mV when human sat or leant on this sponge.

4. Summary and perspectives

The rapid development of TE materials and their devices has attracted tremendous interests because of their great potential in applications such as next-generation power generator, self-powered wearable electronics, as well as power supply for various external powered portable electronics. Aerogels-based conducting materials possess attractive ultralow κ, light weight and adjustable σ, enabling them as a highly promising candidate to effectively achieve the heat-to-electricity conversion. In this article, we have introduced the recent progress of organic, inorganic and composite/hybrid TE aerogels, including main constituents, preparation approach, TE performance and factors affecting the TE performance and the corresponding mechanism. We have also presented two representative aerogel-based TE devices/generators, and further discussed their assembly mode and TE output performance. Although remarkable progress has been achieved for the TE aerogels, research in this field is still in the infancy stage, especially compared with those organic or inorganic based TE films or bulks. The future research of TE aerogels and their devices could be focused on the following aspects.

1) For 3D TE aerogels, it remains a great challenge to simultaneously improve the σ and reduce/remain low κ, especially compared to the corresponding TE films. The optimization methods (doping, de-doping, pre-/post-treatment), morphology and structure control (1D nanowires or nanotubes, 2D nanosheets, 3D nanospheres, ordering of polymer chains, orientation), as well as the enhancement mechanisms (synergistic effect, energy-filtering effect, phonon scattering effect) of some films or bulk materials with high TE properties can be used to optimize the preparation and TE performance of TE aerogels.

2) Highly elastic TE aerogels. Considering the porous structure of aerogels and the practical applications, TE aerogels with high elasticity will exhibit unique advantages. Combing the high elasticity of conventional aerogels with the desired TE property of TE materials (carbon nanoparticles, conducting polymers, semiconductors), a highly elastic TE aerogel is expected to be achieved. Some feasible strategies mainly include: the optimization of preparation process, elastic material as matrix together with some treatments (coating, dipping, vapor phase polymerization, etc), as well as the construction of multicomponent system.

3) Optimization of aerogel-based TE devices. Considering the advantages of ultra-light weight and low κ of TE aerogels, they can be designed into devices in vertical mode to broaden their application scenarios (floating in hot fluid medium, wearable/portable devices). Moreover, high elasticity and/or high flexibility can be applied to prepare compressible and/or stretchable TE devices.

4) In particular, in-depth understanding of the enhancement mechanism of the TE aerogels needs to be emphasized. Besides the 3D conductive network, energy-filtering effect and phonon scattering effect employed from TE materials films/bulks, novel concepts or theories are need to be provided to accurately clarify the variation of TE performance, so as to further optimize the performance of the TE aerogels.

Acknowledgements

Project supported by Shenzhen Fundamental Research Program (Grant No. JCYJ20200109105604088) and Distinguished Young Talents in Higher Education of Guangdong, China (Project No. 2020KQNCX061).

References

[1] Fan Z, Zhang Y, Pan L, Ouyang J and Zhang Q 2021 *Renew. Sust. Energ. Rev.* **137** 110448
[2] Liang L, Lv H, Shi X L, Liu Z, Chen G, Chen Z G and Sun G 2021 *Mater. Horiz.* **8** 2750
[3] Liu Z and Chen G 2020 *Adv. Mater. Technol.* **5** 2000049
[4] Lv H, Liang L, Zhang Y, Deng L, Chen Z, Liu Z, Wang H and Chen G 2021 *Nano Energy* **88** 106260
[5] Zhang Y, Zhang Q and Chen G 2020 *Carbon Energy* **2** 408
[6] Zheng Y, Zeng H N, Zhu Q and Xu J W 2018 *J. Mater. Chem. C* **6** 8858
[7] Yao H, Fan Z, Cheng H, Guan X, Wang C, Sun K and Ouyang J 2018 *Macromol. Rapid Commun.* **39** e1700727
[8] Zhang L, Shi X L, Yang Y L and Chen Z G 2021 *Mater. Today* **46** 62
[9] Jiang Q, Sun H, Zhao D, Zhang F, Hu D, Jiao F, Qin L, Linseis V, Fabiano S, Crispin X, Ma Y and Cao Y 2020 *Adv. Mater.* **32** e2002752
[10] Xiong J, Wang L, Xu J, Liu C, Zhou W, Shi H, Jiang Q and Jiang F 2015 *J. Mater. Sci. Mater. Electron.* **27** 1769
[11] Hong M, Chen Z G and Zou J 2018 *Chin. Phys. B* **27** 048403
[12] Zhai J, Wang T, Wang H, Su W, Wang X, Chen T and Wang C 2018 *Chin. Phys. B* **27** 047306
[13] Deng L and Chen G 2021 *Nano Energy* **80** 105448
[14] Bharti M, Singh A, Samanta S and Aswal D K 2018 *Prog. Mater. Sci.* **93** 270
[15] Wang X, Meng F, Tang H, Gao Z, Li S, Jin S, Jiang Q, Jiang F and Xu J 2018 *Synth. Met.* **235** 42
[16] Fan J, Huang X, Liu F, Deng L and Chen G 2021 *Compos. Commun.* **24** 100612
[17] Chen X, Shi W and Zhang K 2020 *ACS Appl. Mater. Interfaces* **12** 34451
[18] Yang J, Jiang Q, Zhang J, Xu J, Liu J, Liu P, Liu G, Wang Y and Jiang F 2020 *Synth. Met.* **269** 116546
[19] Jiang Q, Lan X, Liu C, Shi H, Zhu Z, Zhao F, Xu J and Jiang F 2018 *Mater. Chem. Front.* **2** 679
[20] Liang L, Fan J, Wang M, Chen G and Sun G 2020 *Compos. Sci. Technol.* **187** 107948
[21] Ni D, Song H, Chen Y and Cai K 2020 *J. Materiomics* **6** 364
[22] Deng W, Deng L, Li Z, Zhang Y and Chen G 2021 *ACS Appl. Mater. Interfaces* **13** 12131
[23] Yin S, Lu W, Wu R, Fan W, Guo C Y and Chen G 2020 *ACS Appl. Mater. Interfaces* **12** 3547
[24] Hu X, Zhang K, Zhang J, Wang S and Qiu Y 2018 *ACS Appl. Energy Mater.* **1** 4883
[25] Wang S, Zhou Y, Liu Y, Wang L and Gao C 2020 *J. Mater. Chem. C* **8** 528
[26] Liu Y X, Liu H H, Wang J P and Zhang X X 2018 *J. Polym. Eng.* **38** 381
[27] Wang Y, Yang J, Wang L, Du K, Yin Q and Yin Q 2017 *ACS Appl. Mater. Interfaces* **9** 20124
[28] Ćirić-Marjanović G 2013 *Synth. Met.* **170** 31
[29] Guo Y, Dun C, Xu J, Li P, Huang W, Mu J, Hou C, Hewitt C A, Zhang Q, Li Y, Carroll D L and Wang H 2018 *ACS Appl. Mater. Interfaces* **10** 33316
[30] Mitra M, Kargupta K, Ganguly S, Goswami S and Banerjee D 2017 *Synth. Met.* **228** 25
[31] El-Shamy A G 2019 *Compos. B. Eng.* **174** 106993
[32] Li Z, Deng L, Lv H, Liang L, Deng W, Zhang Y and Chen G 2021 *Adv. Funct. Mater.* **31** 2104836
[33] Zhang Y, Deng L, Lv H and Chen G 2020 *npj Flex. Electron.* **4** 26
[34] Lee J H and Park S J 2020 *Carbon* **163** 1
[35] Wang X, Liu P, Jiang Q, Zhou W, Xu J, Liu J, Jia Y, Duan X, Liu Y, Du Y and Jiang F 2019 *ACS Appl. Mater. Interfaces* **11** 2408
[36] Zhao X, Wang W, Wang Z, Wang J, Huang T, Dong J and Zhang Q 2020 *Chem. Eng. J.* **395** 125115
[37] Jia F, Wu R, Liu C, Lan J, Lin Y H and Yang X 2019 *ACS Sustainable Chem. Eng.* **7** 12591
[38] Kim J, Bae E J, Kang Y H, Lee C and Cho S Y 2020 *Nano Energy* **74** 104824
[39] Blackburn J L, Ferguson A J, Cho C and Grunlan J C 2018 *Adv. Mater.* **30** 1704386
[40] Yang J, Yip H L and Jen A K Y 2013 *Adv. Energy Mater.* **3** 549
[41] Wang L, Yao Q, Shi W, Qu S and Chen L 2017 *Mater. Chem. Front.* **1** 741
[42] Long Y Z, Li M M, Gu C, Wan M, Duvail J L, Liu Z and Fan Z 2011 *Prog. Polym. Sci.* **36** 1415
[43] Zhang Z, Liao M, Lou H, Hu Y, Sun X and Peng H 2018 *Adv. Mater.* **30** e1704261
[44] Gueye M N, Carella A, Faure-Vincent J, Demadrille R and Simonato J P 2020 *Prog. Mater Sci.* **108** 100616
[45] Fan Z and Ouyang J Y 2019 *Adv. Electron. Mater.* **5** 1800769
[46] Kim G H, Shao L, Zhang K and Pipe K P 2013 *Nat. Mater.* **12** 719
[47] Gordon M P, Zaia E W, Zhou P, Russ B, Coates N E, Sahu A and Urban J J 2017 *J. Appl. Polym. Sci.* **134** 44070
[48] Yanagishima N, Kanehashi S, Saito H, Ogino K and Shimomura T 2020 *Polymer* **206** 122912
[49] Okada N, Sato K, Yokoo M, Kodama E, Kanehashi S and Shimomura T 2020 *ACS Appl. Polym. Mater.* **3** 455
[50] Acharyya P, Kundu K and Biswas K 2020 *Nanoscale* **12** 21094
[51] Ganguly S, Zhou C, Morelli D, Sakamoto J and Brock S L 2012 *J. Phys. Chem. C* **116** 17431
[52] Adekoya G J, Sadiku R E and Ray S S 2021 *Macromol. Mater. Eng.* **306** 2000716
[53] Chen J, Gui X, Wang Z, Li Z, Xiang R, Wang K, Wu D, Xia X, Zhou Y, Wang Q, Tang Z and Chen L 2012 *ACS Appl. Mater. Interfaces* **4** 81
[54] Zhao L, Sun X, Lei Z, Zhao J, Wu J, Li Q and Zhang A 2015 *Compos. B. Eng.* **83** 317
[55] Gupta S and Meek R 2020 *Appl. Phys. A* **126** 704
[56] Tan D, Zhao J, Gao C, Wang H, Chen G and Shi D 2017 *ACS Appl. Mater. Interfaces* **9** 21820
[57] Lei Z, Yan Y, Feng J, Wu J, Huang G, Li X, Xing W and Zhao L 2015 *RSC Adv.* **5** 25650
[58] Sun X, Zhao J, Zhao L, Wu J and Li Q 2016 *RSC Adv.* **6** 109878
[59] Wang L, Bi H, Yao Q, Ren D, Qu S, Huang F and Chen L 2017 *Compos. Sci. Technol.* **150** 135
[60] Qi X, Miao T, Chi C, Zhang G, Zhang C, Du Y, An M, Ma W G and Zhang X 2020 *Nano Energy* **77** 105096
[61] Sun X, Wei Y, Li J, Zhao J, Zhao L and Li Q 2017 *Sci. China Mater.* **60** 159
[62] Gnanaseelan M, Chen Y, Luo J, Krause B, Pionteck J, Pötschke P and Qi H 2018 *Compos. Sci. Technol.* **163** 133